Using α-chitin nanocrystals to improve the final properties of poly (vinyl alcohol) films with Origanum vulgare essential oil

Rut Fernández-Marín, Jalel Labidi, María Ángeles Andrés, Susana C.M. Fernandes

Using α-chitin nanocrystals to improve the final properties of poly (vinyl alcohol) films with *Origanum vulgare* essential oil

Rut Fernández-Marín[1], Jalel Labidi[1], María Ángeles Andrés[1*], Susana C.M. Fernandes[2*]

[1]Environmental and Chemical Engineering Department, University of the Basque Country UPV/EHU, Plaza Europa 1, 20018, Donostia-San Sebastián, Spain.

[2] Université de Pau et des Pays de l'Adour, E2S UPPA, CNRS, IPREM, 64600 Anglet, France.

Corresponding to:

Susana C.M. Fernandes: susana.fernandes@univ-pau.fr

María Ángeles Andrés: marian.andres@ehu.eus

Abstract

In the present work, nanocomposite films based on poly(vinyl alcohol) (PVA) containing different amounts of Origanum vulgare essential oil (OEO, 0, 0.5, 1, 1.5 and 2% v/v) were reinforced with 0.5 % (w/v) of alpha chitin nanocrystals (α-CHNC, from shrimp and from lobster) and prepared by solvent casting. Another set of films was prepared without α -CHNC to assess the effect of the nanocrystals on the final properties of the films. The obtained nanocomposite films were homogeneous and showed better thermal stability and mechanical properties. After exposure the nanocomposite films to ultraviolet radiation, the obtained data revealed that the presence of α-CHNC into the materials has a retarding effect on their loss of mechanical properties. It was also shown that the antioxidant activity and the total phenolic content of the materials increased with the augmentation of OEO and with the antioxidant

release time. Interestingly, the nanocomposite films made of chitin nanocrystals from shrimp showed better total phenolic content than the unfilled films and the nanocomposite films made of chitin nanocrystals from lobster over the first 48h. Henceforward, this study demonstrated the potential of the nanocomposite films based on PVA, OEO and reinforced with α-CHNC for active food-packaging applications.

Keywords

Chitin nanocrystals, poly(vinyl alcohol), oregano oil, nanocomposite films, mechanical properties, antioxidant activity

1. Introduction

One of the big challenges for our society in this century is to decrease the enormous amount of non-biodegradable plastics waste. Every year, 150 million tons of plastic waste are estimated to reach the oceans [1].

To replace part of these non-biodegradable plastics for biodegradable and/or 'bioplastics', *i.e.* plastics prepared from renewable resources (biopolymers), in recent years, many by-products from both agricultural and marine companies have gained interest in different industry sectors such as cosmetics, medical and food packaging due to their sustainable and eco-friendly attributes. Therefore, numerous scientific studies have been done in this sense. This include the use of natural polymers or synthetic biodegradable polymers that can be use as matrices and/or reinforcing agents; and bioactive compounds, which are used to improve the biological properties of the final materials.

Among the polymers, chitin (poly(β-(1-4)-N-acetyl-D-glucosamine), is a biopolymer found in the exoskeleton of crustaceans like crabs, lobster and shrimps; and is one of the biggest residues in fishing industry [2,3]. However, it can also be found in the cell walls of fungi and in cuticle of insects. Being a supporting material in nature, chitin presents a highly organized micro- and nano-fibrillated structure. Under acid hydrolysis it is possible to obtain chitin nanocrystals (CHNC) with dimensions that can range from 6-60 nm in width and 100-800 nm in length [4,5]. These chitin nanocrystals present excellent properties namely low density, biocompatibility, low toxicity, biodegradability and antimicrobial properties. In addition, its use as reinforcement agents in biocomposite films, improves the thermal stability and the mechanical properties [6,7]. A very interesting synthetic polymer, that can be used for the mentioned applications, is poly(vinyl alcohol), PVA. It is a biodegradable, non-toxic, biocompatible and soluble in water polymer presenting good film-forming and mechanical properties [8–10].

Among the bioactive agents, essential oils (EOs) are one of the most important products of agriculture-based industry due to its bioactive properties that include antimicrobial, antiviral, antioxidant, anticancer and immunomodulatory [11–13]. Their production is superior to 70,000 tons per year. EOs are aromatic compounds with low molecular weight extracted from plants namely barks (cinnamon), leaves (eucalyptus), flowers (lavender) and peels of fruits (orange) [12,14]. They possess various applications in health, agriculture, cosmetic, food and medicine industries. Moreover, are recognized by the Generally Recognized as Safe (GRAS) by the US Food and Drug Administration (USFDA) as safe foods [11]. Due to its medicinal and culinary properties, oregano essential oil (*Origanum vulgare),* which belongs to the *Lamiaceae*

family, is one of the most employed oil since ancient times. Its properties are attributed to the presence of monoterpenes among which carvacrol and thymol stand out [15,16].

The use of EOs is quite limited because of their high volatile properties and easily decomposition during handling, heating, exposure to oxygen or ultraviolet light, etc. [17,18]. For these reasons, EOs need to be encapsulated/incorporated in materials that could present the form of films, coatings, nanocapsules and emulsions, in order to preserve their bioactive activities. Therefore, different polymeric matrices have been used such as chitosan, polylactic acid (PLA), soy protein, fish gelatine among others [19–22]. For instance, Munhuweyi *et al.* [23] used chitosan as matrix with oregano oil, and Wu J. *et al.* [24] used a mixture of gelatine with chitosan by incorporating this oil to make films. Also, PVA films were developed by mixing this polymer with clove oil and apple pomace as bioactive agents [9,10,25,26,27]. Hashemi *et al.* [27] prepared a basil seed gum coating with oregano oil and Fraj *et al.* [28] obtained polycaprolactone nanocapsules using this oil as an active ingredient. On the other hand, Hosseini et al. [16] studied emulsions of chitosan with oregano oil and Ribes et al. [29] prepared an emulsion with clove and oregano oil mixed with xanthan gum.

Nonetheless, there are few works in which nanocrystals or nanofibers like nanocellulose or nanochitin, have been used to reinforce the final mechanical and biological properties of the films. Some examples are the research done by Luzi *et al*. [31] where the authors used PVA and chitosan, as a matrix adding carvacrol, as bioactive agent and cellulose nanocrystals as reinforcing agent; or by Ardekani *et al.* [30] that assessed the properties of PVA, *Zataria multiflora* oil and mats nanofiber films; or by Jahed *et al.* [32] that studied the physicochemical properties of *Carum copticum* essential oil loaded chitosan films containing organic nanoreinforcements.

In this context, the aim of this research was to developed bioactive nanocomposite films using two different sources of alpha-chitin nanocrystals (α-CHNC) as reinforcing agents to improve the final properties of PVA and *Origanum vulgare* essential oil (OEO) films. To the best of our knowledge, chitin nanocrystals have not been studied as reinforcing agents in PVA with EOs, in particular with oregano oil. The effect of the different concentrations of EO and the origin of chitin nanocrystals on the final properties of the nanocomposite films, were assessed. Therefore, their thermal, mechanical and antioxidant properties were studied in order to evaluate their potential use in food packaging applications.

2. Materials and methods

2.1. Materials

Two different chitin samples were used, one was kindly provided by Mahtani Chitosan Pvt. Ltd. (India), and the other, was extracted *in-house* from lobster exoskeletal waste that was kindly supplied by Antarctic Seafood S.A. (Chile). The two chitin nanocrystal samples were isolated in-house with the mentioned chitin samples by microwave irradiation technique (CEM-Discover) at 125 w for 10 min using a 1 M HCl solution (37 % w/w, ACS reagent) in order to hydrolyse the amorphous regions of the chitin. The ratio chitin: HCl was of 1:30 w/v as described by Salaberria et al. [5]. After, the suspensions were cooled at room temperature, filtered, washed with distilled water until neutral pH and centrifuged in order to remove the excess of water. The two like-gel samples were finally stored in a refrigerator at 4 °C. These two chitin samples were then characterized. The degrees of acetylation (DA), determined by solid ^{13}C NMR using a Bruker Advance III 400 spectrometer (USA), determined according Kasaai *et al.* [33] and were found to be 85% and 90% for shrimp and lobster chitin nanocrystals,

respectively. The crystallinity index (CI%), was 89% for shrimp chitin nanocrystals and 94% for lobster chitin nanocrystals, as obtained by X Ray Diffraction (XRD) spectra (Philip X'pert Pro Automatic diffractometer, Amsterdam, Netherlands), using the published Sagheer et al. [34] equation.

Oregano oil FCC (OEO*, Origanum vulgare,* with Food Grade) was supplied by Sigma-Aldrich. *Origanum vulgare* essential oil composition was determined using gas chromatography and mass spectrometry (GC/MS, Agilent GC 7890A, MS 5975C, USA). Briefly, 10 µL of oregano oil were dissolved in 1 mL of ethyl acetate and injected in a capillary column HP-5MS ((5 %-Phenyl) - methylpolysiloxane, 30 m x 0.25 mm). The GC/MS conditions were: split/splitless method in split mode (10:1), injector at 280 °C and Helium was used as carrier gas at a flow rate of 0.7 mL/min. The rate temperature began at 50 °C and was increased until 120 ˚C at 10 K/min and held for 5 min. In a second time, the temperature was raised to 280 ˚C at 10 K/min and holds this temperature during 8 min. And, finally, the temperature was increased to 300 ˚C at 10 K/min and held for 2 min. The identification of the different compounds was carried out by using the National Institute of Standards Library (NIST). The obtained data is summarized in the Table 1. Only compounds with areas superior to 0.4 were accounted for. 14 compounds of OEO were identified representing 97.4% of the total essential oil. The main components were carvacrol representing 75% and ϒ-terpinene at around 5.96%. These results are in agreement with those obtained previously by Munhuweyi et al. [23] and Hosseini et al. [16].

Table 1. Composition of Origanum vulgare assessed by GC/MS.

Component	**Area (%)**	**Retention Time (min)**

1R-α-Pinene	0.51	5.07
β-Pinene	0.40	5.69
β-Myrcene	0.56	5.81
α-Terpinene	0.92	6.24
o-cymenene	5.87	6.36
Eucalyptol	0.60	6.47
γ-Terpinene	5.96	6.86
β-Linalool	1.46	7.44
Borneol	0.82	8.76
1-terpinen-4-ol	0.52	8.98
Thymol	1.97	11.99
Carvacrol	75.05	12.50
Caryophyllene	2.33	15.55
α-Humulene	0.43	16.22
Total	**97.4**	-

Hydrochloric acid (HCl 37%, ACS reagent), ethanol (EtOH, analytical standard), methanol (MeOH, HPLC grade), ethyl acetate (HPLC grade), Poly(vinyl alcohol) (PVA, Mw 13 000-23 000, 87-89% hydrolysed), Trolox (6-Hydroxy-2,5,7,8-tetramethylchromane-2-carboxylic acid, 97 %) and DPPH (2,2-diphenyl-1-picrylhydrazyl) were supplied by Sigma-Aldrich. Gallic acid monohydrate (extra pure) and Folin-Ciocalteu reagent were purchased from Scharlau. Sodium carbonate anhydrous (general-purpose grade) was purchased from Fischer.

2.2. Preparation of the nanocomposite films

PVA solutions (2% w/v) were prepared by dissolving PVA in a mixture of ethanol (60% v/v) and distilled water under stirring overnight at 55 ˚C. The oregano essential oil (OEO) concentration varied from 0.5 to 2% v/v with respect to PVA solution. The nanocomposite films were prepared by adding 0.5% w/v of chitin nanocrystals (α-CHNC, from shrimp or lobster). The dispersion of α-CHNC in the PVA solutions was done using an Ultra-Turrax (Heidolph Silent Crusher M., Germany) at 13 500 rpm for 10 min. A second set of samples was prepared without α-CHNC. All suspensions or solutions were degassed in order to remove entrapped air. The films were then prepared by casting at room temperature using 50 mm-diameter silicon molds for 72 hours. The ensuing materials were kept in a conditioning cabinet at 50 ± 5% relative humidity (RH) and 25 °C.

In order to assess the impact of the ultraviolet (UV) irradiation on the nanocomposite films, the samples were exposed to UV light into a dark room with an UV lamp at 364 nm during 3 days according to the method described by Morales *et al*. [8]. The effect of the UV irradiation was evaluated by measuring the mechanical properties of the films.

The identification and composition of the nanocomposite films in terms of α-CHNC and OEO are listed in Table 2.

Table 2. Identification and composition of the nanocomposite films.

Samples identification	**Source of α - CHNC**	**PVA (% w/v)**	**α-CHNC (% w/v)**	**OEO (% v/v)**
P-0	-	2	0	0
P-0.5		2	0	0.5

P-1		2	0	1
P-1.5		2	0	1.5
P-2		2	0	2
PNCS-0		2	0.5	0
PNCS-0.5		2	0.5	0.5
PNCS-1	**Shrimp**	2	0.5	1
PNCS-1.5		2	0.5	1.5
PNCS-2		2	0.5	2
PNCL-0		2	0.5	0
PNCL-0.5		2	0.5	0.5
PNCL-1	**Lobster**	2	0.5	1
PNCL-1.5		2	0.5	1.5
PNCL-2		2	0.5	2

2.3. Characterization of nanocomposite films

2.3.1. Physico-chemical characterization

A UV-Vis spectrophotometer (Jasco V-630 UV-VIS spectrophotometer, JASCO, Germany) was used to assess the transmittance of the films. Spectra were recorded at RT in steps of 1 nm in the 400 −750 nm range. The measurements were made in triplicate.

The opacity of each films was determined according to the method described by Priyadarshi et al. [35]. The opacity was determined by equation (Eq. 2):

$$Opacity = \frac{Abs_{600}}{x} \qquad \text{(Eq. 2)}$$

Where Abs 600 represents the absorbance obtained at 600 nm and x is the thickness of the film (mm). The thickness of the nanocomposite films was measured using a digital micrometer (Ultra Präzision Messzeuge GmbH, Glattbach, Germany) with an accuracy of 0.001 mm in six random different points of the each film. The average thickness was then calculated.

Attenuated Total Reflection-Fourier Transform Infrared Radiation (ATR-FTIR) analysis was used to study the chemical interactions between PVA, OEO and α-CHNC using a Spectrum Two FTIR Spectrometer (Perkin Elmer Inc., Waltham, MA, USA) with a Universal Attenuated Total Reflectance accessory. The range of transmittance was between 600 and 4000 cm^{-1} using 64 scans and 4 cm^{-1} of resolution.

The moisture content of the nanocomposite films was determined by adapting the method described by [18]. Prior to testing, all samples were cut in 1.5 x 3 cm^2 models. Afterwards, the samples were weighed and dried at 106 ˚C for 24 h in an oven (Memmert UN160 plus Twindisp, Germany) to attain a constant weight. The moisture content was determined according to the following equation:

$$\text{Moisture content } (\%) = \frac{(W1-W2)}{W2} x\ 100 \qquad \text{(Eq. 1)}$$

Where W1 is the initial weight of the sample (g) and W2 is the weigh after drying (g). Three measurements were conducted for each sample and their average was calculated.

2.3.2. Thermal stability and mechanical properties of the nanocomposite films

The thermal stability of the films was determined by thermogravimetric analysis (TGA) using a TGA/SDTA 851 Mettler Toledo instrument (New Castle, DE, USA), at a scanning rate of 10°C/min, from room temperature to 750 °C under a nitrogen atmosphere.

The mechanical properties of the nanocomposite films were performed using an Instron 5967 tester (Instron, Norwood, MA, USA). A load cell of 50 N was used with a cross head speed of 3 mm/min. Eight replicates of each sample (0.5 cm x 4.5 cm, L x W) were used to determine the average values of Young's modulus, tensile strength and elastic modulus.

2.3.3. Antioxidant activity

Determination of the total phenolic content (TPC)

The total phenolic content of the nanocomposite films was determined according to the method described by Ruiz-Navajas *et al.* [3]. 25 mg of each film were cut and dissolved in 3 mL of methanol and centrifuged at 300 rpm for 12, 24, 48 and 72h. Then, the supernatant was collected and for each extract 300-µL solution was employed. Gallic acid was used as reference standard and the measurement was done at 760 nm using a UV-Vis spectrophotometer (Jasco V-630, Pfungstadt, Germany). The results were expressed as mg gallic acid equivalents (GAE)/ g of dried film. Each sample was tested in triplicate.

DPPH (2,2-diphenyl-1-picrylhydrazyl) radical scavenging assay

The antioxidant activity of the nanocomposite films was evaluated using a free radical scavenging assay DPPH (2, 2-diphenyl-1-picrylhydrazyl) according to the method described by Gullon *et* al. [36] with slight modifications. 25 mg of each film were cut and dissolved in 3 mL of methanol and centrifuged at 300 rpm for 12, 24, 48 and 72h. Then, the supernatant was collected. Afterwards, 300 µL of film extracts were mixed with 3 mL of $6x10^{-5}$M methanol solution of DPPH. After 15 min, the decrease in absorbance was measured at 515 nm using a UV-Vis spectrophotometer (Jasco V-630, Pfungstadt, Germany). Trolox was applied as standard reference and the results were

expressed in μmol of Trolox equivalent (TE)/ g of dried film. Each sample was measured in triplicate.

2.4. Statistical analysis

The statistical analysis was performed using one-way analysis of variance (ANOVA) by SPSS software (Version 24, Inc. Chicago, IL, USA). The values of the significant differences were determined by Duncan's multiple range test. The experiments were carried out at least three times for each condition. The results are expressed as Mean±SD and values of $p<0.05$ were considered to be statistically significant.

3. Results and discussion

3.1. Physico-chemical characterization of the nanocomposite films

Our main aim in this study was to developed bioactive nanocomposite films using two different sources of alpha-chitin nanocrystals (α-CHNC) as reinforcing agents to improve the final properties of PVA and *Origanum vulgare* essential oil (OEO) films. Herein, we specifically focus on the effect of the different concentrations of OEO and the origin of chitin nanocrystals on the final properties of the PVA-based nanocomposite films. As a first step, we focused on the general aspect of the films and on their physicochemical characterization. Afterwards, their thermal and mechanical properties, as well as their stability against UV light and their antioxidant properties were assessed in order to evaluate their potential use for packaging-food applications.

One of the most important parameters in films for food applications is their transparency because it has a direct impact on the consumer acceptance. To evaluate the impact of the incorporation of OEO and chitin nanocrystals on the transparency of the

final materials, pictures were taken and the transmittance and opacity of the nanocomposite films were measured and calculated, respectively.

Figure 1, displays the general aspect of the final films. The obtained films are homogeneous and translucent. Figure 2 represents the transmittance (measured in the range between 400 -750 nm) profiles of the nanocomposite films and confirms the qualitative analyse of Figure 1.

Figure 1. General appearance of the nanocomposite films. From left to right: a) P-O, P0.5/P1/P1.5/P2; b) PNCS-O/PNCS-0.5/PNCS-1/PNCS-1.5/PNCS-2; c) PNCL-O/PNCL-0.5/PNCL-1/PNCL-1.5/PNCL-2.

As demonstrated in Figure 2, in the range of the visible light (400 to 750 nm), the highest transmittance were ascribed to the unfilled PVA film (P-0, around 90 % at 600 nm) and to the films prepared with low concentrations of OEO. However, our data showed that the incorporation of high concentration of OEO (P-2) decreases the transmittance of the films. On the other hand, as expected, the addition of chitin nanocrystals decreases the transmittance of the nanocomposite films (PNCS-0 and

PNCL-0), as previously demonstrated with other matrices [5,37]. Interestingly, the incorporation of OEO into the nanocomposite films showed a decrease of the transmittance of the final materials. Previous studies, have demonstrated the influence of the addition of EOs on different matrices, namely the work described by Sahraee et al. [18] and Gomes et al. [38], where the authors prepared materials using chitosan as matrix with different concentrations of essential oils; or described by Kanatt et al. [39], where chitosan and PVA were blended with plants extract.

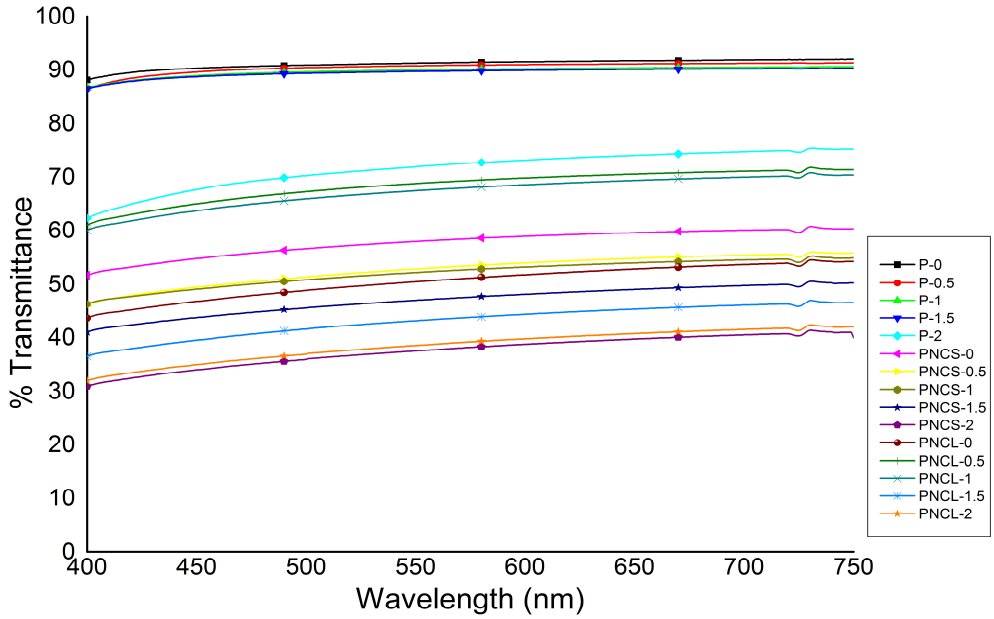

Figure 2. Transmittance from 400 to 750 nm of the nanocomposites films.

To underline these data, the opacity of the films was also calculated (equation 2, that take in account the Absorbance of the films at 600 nm and the thickness). The results are listed in Table 3. The lowest opacity value was observed in the pure PVA film (P-0) presenting an opacity of 0.65 ± 0.01. Similar to the data obtained by Chen et al. [9], by incorporating clove essential oil or apple pomace into PVA films, the opacity

of our nanocomposite films increases with the incorporation of high concentrations of OEO (P-1.5 and P-2). In addition, the addition of nanocrystals resulted in a consequent increase of the opacity of the films. No significant differences were observed between the 2 types of chitin nanocrystals: 2.16 to 2.99 and 2.43 to 2.84 for films prepared with shrimp and lobster chitin nanocrystals, respectively.

Table 3. Data concerning the thickness, opacity and moisture content of the nanocomposite films.

The values were average ± standard deviation (thickness n=6; moisture content and opacity n=3). Superscript letters depict significant differences (Duncan's test, $p < 0.05$) among OEO concentration with in each chitin nanocrystals treatment.

Samples Identification	**Thickness (µm)**	**Opacity**	**Moisture content (%)**
P-0	48.0 ± 1.8^{a}	0.65 ± 0.01^{a}	11.0 ± 0.2^{a}
P-0.5	49.0 ± 3.5^{a}	0.66 ± 0.02^{a}	10.8 ± 0.8^{a}
P-1	60.2 ± 3.6^{b}	0.68 ± 0.06^{a}	8.0 ± 0.1^{b}
P-1.5	66.7 ± 2.3^{c}	0.75 ± 0.02^{b}	5.9 ± 0.7^{c}
P-2	72.8 ± 2.0^{d}	0.93 ± 0.04^{c}	5.1 ± 0.2^{d}
PNCS-0	48.2 ± 2.1^{a}	2.16 ± 0.12^{a}	13.2 ± 3.2^{a}
PNCS-0.5	53.2 ± 2.0^{b}	2.36 ± 0.34^{ab}	10.0 ± 2.7^{a}
PNCS-1	56.2 ± 3.0^{b}	2.38 ± 0.05^{ab}	9.1 ± 1.2^{a}
PNCS-1.5	61.8 ± 3.8^{c}	2.44 ± 1.94^{b}	7.7 ± 2.9^{a}

PNCS-2	64.3 ± 3.8^{c}	2.99 ± 0.19^{b}	7.4 ± 1.9^{a}
PNCL-0	51.1 ± 4.3^{a}	2.43 ± 1.40^{a}	13.1 ± 0.5^{a}
PNCL-0.5	65.1 ± 1.1^{b}	1.96 ± 0.04^{b}	11.4 ± 1.3^{ab}
PNCL-1	71.2 ± 3.0^{c}	2.14 ± 0.07^{c}	10.4 ± 1.6^{b}
PNCL-1.5	76.0 ± 4.8^{cd}	2.56 ± 0.04^{d}	8.1 ± 0.5^{c}
PNCL-2	79.2 ± 5.8^{d}	2.84 ± 1.64^{e}	6.0 ± 0.4^{d}

Another important aspect for food-packaging materials is their water absorbance capacity, because being in contact with food can cause the damage of the product. Table 3 reports the results of the moisture content of the nanocomposite films. The data listed in Table 3 show that the incorporation of OEO decreases the moisture content of the PVA films. The lowest value of moisture content was observed for the P-2 films (5.1 ± 0.2%). Interestingly, even for the nanocomposite films that have an important amount of OH groups, the incorporation of OEO induces the decrease of moisture content. These results are attributed to the hydrophobic properties of the OEO, and good interaction between OEO, α-CHNC and PVA leaving least possibility for them to interact with water molecules [40].

In Table 4 are listed the ATR-FTIR band assignments of OEO and PVA. For instance, the OEO spectra presented a broad peak at 3397 cm^{-1} corresponding to the O-H stretching which was attributed to carvacrol, and the phenolic ring was assigned to the peaks between 1622 and 1424 cm^{-1}. The peak at 941 cm^{-1} showed C-H bending and at 810 cm^{-1} revealed the characteristic peak of thymol [28,30].

Regarding the PVA, for example, the peaks at 1732 cm^{-1} and 1573 cm^{-1} were attributed to ester C=O stretching vibration and C=C stretching vibration, respectively. Other representative bands of PVA are the C-C stretching vibration at 1090 cm^{-1} and

1022 cm^{-1}, and C-C and C-O stretching vibration at 843 cm^{-1} [30,41]. In addition, the C-H_2 bending vibration and C-CH_3 deformation vibration were observed at 1428 cm^{-1} and 1377 cm^{-1}, respectively [8,25,42].

Table 4. ATR-FTIR band assignments of OEO and PVA.

	Band (cm^{-1})	**Functional group assignment**
OEO	3397	O-H stretching
	2960	symmetric C-H stretching
	2872	asymmetric C-H stretching
	1622 - 1424	phenolic ring
	1586	N-H bending
	1456	C-H_2 bending
	1250 - 1112	C-O-C stretching
	941	C-H bending
PVA	3295	O-H tensile vibration
	2914 - 2943	alkyl asymmetric stretching
	1732	ester C=O stretching vibration
	1573	C=C stretching vibration
	1428	C-H_2 bending vibration
	1377	C-CH_3 deformation vibration
	1247	C-O stretching
	1090 - 1022	C-C stretching vibration
	843	C-C and C-O stretching vibration

Figure 3, displays the ATR-FTIR spectra of OEO, PVA, PNCS-2 and PNCL-2. All nanocomposite films (not showed) showed characteristics bands corresponding to each component, as demonstrated with the representative examples. For instance, when compared to OEO, P-0 and P-2 spectra, the PNCS-2 and PNCL-2 spectra, showed an increase of the intensity of the band corresponding to the O-H stretching vibrations (around 3400 cm^{-1}); of the bands corresponding to the C-H stretching (around 2950 cm^{-1}); and of the bands at 1657 and 1620 cm^{-1} attributed to amide I and at 1556 cm^{-1}, corresponding to amide II, which is due to the presence of the chitin nanocrystals.

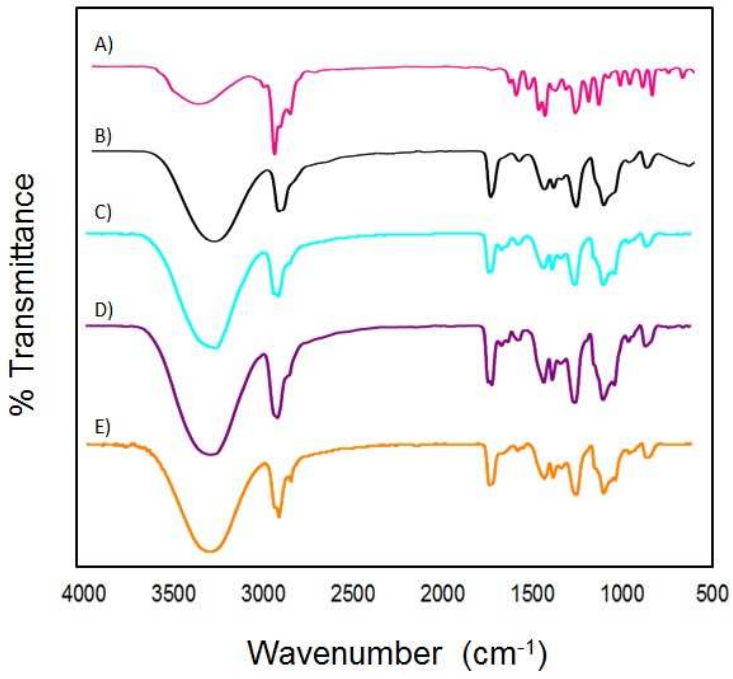

Figure 3.FTIR spectrum of a) OEO, b) P-0, c) P-2, d) PNCS-2, e) PNCL-2.

3.2. Thermal and mechanical properties of the nanocomposite films

The effect of the incorporation of chitin nanocrystals into the PVA/OEO films was evaluated in terms of thermal and mechanical properties. The TGA serves as a proof for chemical interactions and the formation of hydrogen bonds in the final

materials. Figure 4 shows the thermogravimetric analysis (TGA) and derivative (dTGA) curves of the PVA and PVA/OEO films and of the nanocomposite films. The results from TGA and dTGA, clearly showed that the PVA film displayed two-stages of degradation a first step with a maximum degradation at 319 °C attributed to the degradation of the amorphous parts of the polymer, and a second step at around 420 °C that corresponds to the degradation of the higher thermal stability crystalline parts. The PVA/OEO films depicted 4 degradation steps and presented lower thermal stability compared to control. The first step occurred at around 100 °C and was attributed to the loss of water; the second step was observed at 180 °C and was ascribed to the degradation of the OEO [26]. The third and fourth steps were attributed to the PVA degradation, but their maximum temperature of degradation decreased between 15-20 °C. Nevertheless, it was observed that the incorporation of both chitin nanocrystals showed an improvement of the thermal stability of the PVA/OEO films. This fact was attributed to the high temperature of degradation of chitin nanocrystals (around 380 °C, degradation of chitin macromolecules) and to the good homogeneity and interactions between the chitin nanocrystals and the PVA, the increasing of crystallinity of PVA molecules in the presence of the chitin nanocrystals is also a possibility. Like for PVA/OEO films, the nanocomposite's dTGA curves exhibited 4 degradation steps. However, the maximum temperature of degradation of the materials increased (for instance, 318 °C for PNCL-1 and -2, Figure 4).

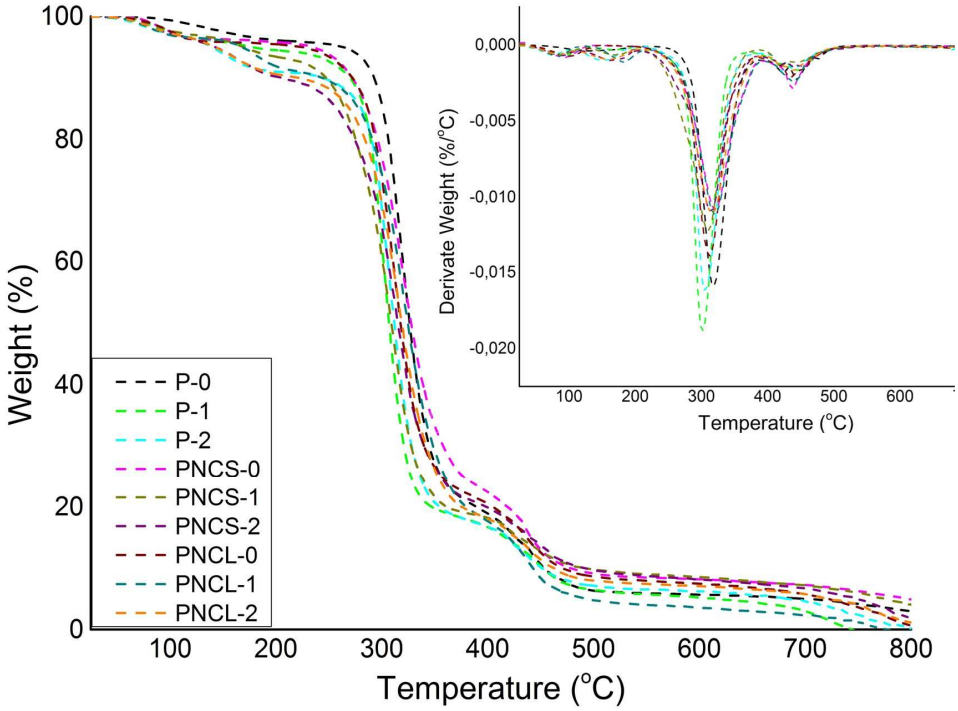

Figure 4. TGA and dTGA curves nanocomposite films: P-0, P-1, P-2, PNCS-0, PNCS-1, PNCS-2, PNCL-0, PNCL-1, and PNCL-2.

The data of the mechanical properties of the nanocomposite films is summarized in Table 5. The results showed no significant differences ($p > 0.05$) regarding the TS values of the unfilled PVA films (without α-CHNC) with the increasing of the concentration of OEO (P-0 to P-2). However, the TS of the nanocomposite films decreased significantly ($p<0.05$) with the concentration of OEO. These results are in accordance with those obtained by Gaikwad et al. [10], in which the TS values decreased with the concentration of apple pomace in PVA films; or with Chen et al. [9] that observed a decrease in TS values in PVA films with clove oil. Nonetheless, the incorporation of the chitin nanocrystals allowed increase the TS with respect to

PVA/OEO films making the nanocomposite films more resistant, as demonstrated before in other matrices [5,43,44].

Table 5. Mechanical properties of the nanocomposite films before and after UV radiation no irradiation and irradiation films (TS: tensile strength; YM: Young's modulus; and E: elongation). The values were average ± standard deviation (n = 10). Superscript letters depict significant differences (Duncan's test, $p < 0.05$) among oil concentration with in each chitin nanocrystals treatment.

	Not UV-irradiated samples			**UV-irradiated samples**		
Samples Identification	**TS (MPa)**	**YM (MPa)**	**E (%)**	**TS (MPa)**	**YM (MPa)**	**E (%)**
P-0	16.02 ± 7.73^{a}	575.61 ± 41.89^{a}	176.44 ± 64.11^{a}	17.68 ± 3.23^{ab}	291.44 ± 93.21^{a}	117.00 ± 10.73^{a}
P-0.5	13.74 ± 1.58^{a}	574.41 ± 5.79^{a}	202.85 ± 72.24^{a}	19.43 ± 1.14^{b}	287.52 ± 98.59^{a}	177.80 ± 6.75^{b}
P-1	14.11 ± 2.71^{a}	555.89 ± 30.84^{a}	224.38 ± 81.11^{a}	12.45 ± 1.82^{a}	260.45 ± 69.77^{a}	172.00 ± 56.87^{b}
P-1.5	14.44 ± 7.43^{a}	512.48 ± 65.98^{a}	295.34 ± 81.89^{b}	11.63 ± 4.95^{a}	243.65 ± 75.53^{a}	186.71 ± 45.93^{b}
P-2	13.06 ± 3.85^{a}	237.99 ± 3.31^{b}	298.97 ± 85.50^{b}	11.44 ± 3.98^{a}	170.89 ± 94.89^{a}	208.51 ± 18.23^{b}
PNCS-0	33.39 ± 2.93^{a}	756.56 ± 197.89^{a}	139.45 ± 82.56^{a}	25.19 ± 4.21^{a}	468.96 ± 179.09^{a}	135.40 ± 38.71^{a}
PNCS-0.5	27.22 ±	579.00 ±	128.73 ±	26.83 ±	454.99 ±	185.70 ±

	2.87[c]	69.85[b]	56.96[a]	1.58[a]	156.37[a]	8.68[ab]
PNCS-1	30.10 ± 2.55[b]	397.89 ± 125.62[c]	195.14 ± 57.95[ab]	21.05 ± 3.89[b]	401.03 ± 112.64[a]	187.29 ± 25.33[b]
PNCS-1.5	23.82 ± 3.70[d]	377.39 ± 91.94[c]	222.83 ± 88.49[b]	16.49 ± 3.21[c]	346.16 ± 117.03[ab]	198.22 ± 51.04[b]
PNCS-2	21.07 ± 1.04[d]	307.85 ± 86.15[c]	225.53 ± 68.78[b]	16.78 ± 2.29[bc]	373.79 ± 102.16[b]	198.53 ± 12.43[b]
PNCL-0	37.88 ± 1.38[a]	754.20 ± 186.71[a]	194.79 ± 29.04[a]	19.79 ± 2.49[a]	487.70 ± 93.21[a]	68.50 ± 18.17[a]
PNCL-0.5	22.52 ± 4.69[b]	385.08 ± 98.10[b]	224.86 ± 60.41[a]	15.24 ± 2.45[b]	322.34 ± 112.59[b]	75.17 ± 9.59[a]
PNCL-1	13.99 ± 1.71[c]	234.18 ± 32.28[c]	214.07 ± 57.73[a]	13.28 ± 2.43[bc]	211.56 ± 69.77[c]	90.24 ± 31.92[a]
PNCL-1.5	12.80 ± 3.11[b]	295.38 ± 57.93[b]	226.33 ± 37.34[b]	12.62 ± 1.95[c]	211.12 ± 75.53[c]	160.03 ± 25.59[b]
PNCL-2	12.67 ± 2.11[c]	242.26 ± 20.97[c]	241.13 ± 43.99[b]	12.35 ± 1.96[c]	186.51 ± 94.89[c]	161.37 ± 72.48[b]

As it could be seen in Table 5, like for TS, no significant differences were observed regarding Young's modulus of PVA films with the OEO concentration. However, the Young's modulus of the nanocomposite films decreased with the OEO concentration; but the incorporation of chitin nanocrystals made that the Young's modulus values are higher PVA/OEO films. Similar results were found by Ardekani et al. [30], the authors used wound dressing of PVA with *Zataria multiflora* oil reinforced

with nanofibers of mats, and used new mats fibers consisting of blend electrospun chitosan / poly (ε-caprolactone) with oregano essential oil.

On the other hand, the addition of the OEO improved the elongation (E %) of the nanocomposite films and consequently their flexibility due to the OEO plasticizing effect [9,45,46].

3.3. Effect of the UV irradiation on the nanocomposite films

The effect of the UV irradiation on the nanocomposite films was assessed by measuring the mechanical properties of the films after irradiation. The samples were exposed to UV light radiation (364 nm) for 72 h and the data are listed in Table 5. No significant changes were observed in the general aspect of the films after the 72 h (images not showed).

In general, comparing the results of the films exposed to UV irradiation with those not irradiated (Table 5), a decrease in mechanical properties was observed. The TS values decreased between 25-50% for the films without α-CHNC and 25-30% for the nanocomposite films.

Rodriguez-Felix et al. [47] observed this trend in chitosan and polyethylene films. With this work, the authors demonstrated that TS values decrease between 80-90 % during 135 days. Other researchers such as Bai et al. [48], showed that after 30 days of exposure to UV light, the values of TS decrease in EDTA/Fe^{3+}/Alginate.

Regarding the Young's modulus results, it was observed that films irradiated during 72 h had lost stiffness since they showed lower values than the films that have not been irradiated. These results are in accordance with Morales et al. [8], which demonstrated that Young´s modulus decreased to 1750 MPa in the bio-oil film when irradiated during 60 h. Furthermore, the Young's modulus values of the films PNCL

(between 468-373 MPa with the content of OEO) were higher than the films PNCS (between 487-186 MPa with OEO concentration). The data also showed that the PNCL nanocomposite films were the ones that showed the highest reduction when they were irradiated with respect to the non-irradiated, observing a drop between 33-67% in their Young´s modulus.

Summarizing, the addition of both α-CHNC as reinforcing agents, for one hand, allowed the increase in mechanical properties of the unfilled PVA/OEO films; and for the other hand, causes an increased of the stability of the final materials when they were submitted to UV radiation.

3.4. Antioxidant activity of the nanocomposite films

In order to avoid the use of synthetic compounds to protect food from oxidation, today there is an increasing demand for active packaging to release natural compounds, in particular essential oils. In this work, to assess the antioxidant activity of the nanocomposite films, two different assays were done: (i) total phenolic content (TPC) used to determine the total amount of phenolic compounds that are important constituents with redox properties responsible for antioxidant activity [49]; and (ii) DPPH assay, in which the antioxidant activity of the samples was measured through the ability of the samples to donate hydrogen to the radical DPPH [50].

Therefore, herein, the profile of total phenolic content and antioxidant release of the OEO from the films and nanocomposite films were studied by immersion in a methanol solution for 12 h, 24 h, 48 and 72 h. The results of the TPC and DPPH assays are shown in Figures 5 and 6, respectively.

In both assays, the pure PVA film (P-0) did not show any antioxidant activity, as demonstrated earlier [25,31]. However, the films prepared with OEO and α-CHNC

showed antioxidant activity. This is consistent with other studies in which it was shown that the OEO contains antioxidant compounds such as carvacrol or thymol [15,16]. Furthermore, the data also demonstrated that the total phenolic content and antioxidant activity of the samples, gradually increased with the increasing of the immersion time and OEO concentration (Figure 5 and 6).

More specifically, regarding to the TPC data (Figure 5), the P-2 film, which contains a higher concentration of OEO, showed the greater release of phenolic compounds with 36.47±0.04 mg GAE/g film value at 72 h. On the other hand, it was observed that in films without nanocrystals there was a huge increase in phenolic content from 12h to 72 h. For instance, for the films P-1, P-1.5 and P-2 an increase of 85%, 78% and 95% was observed, respectively.

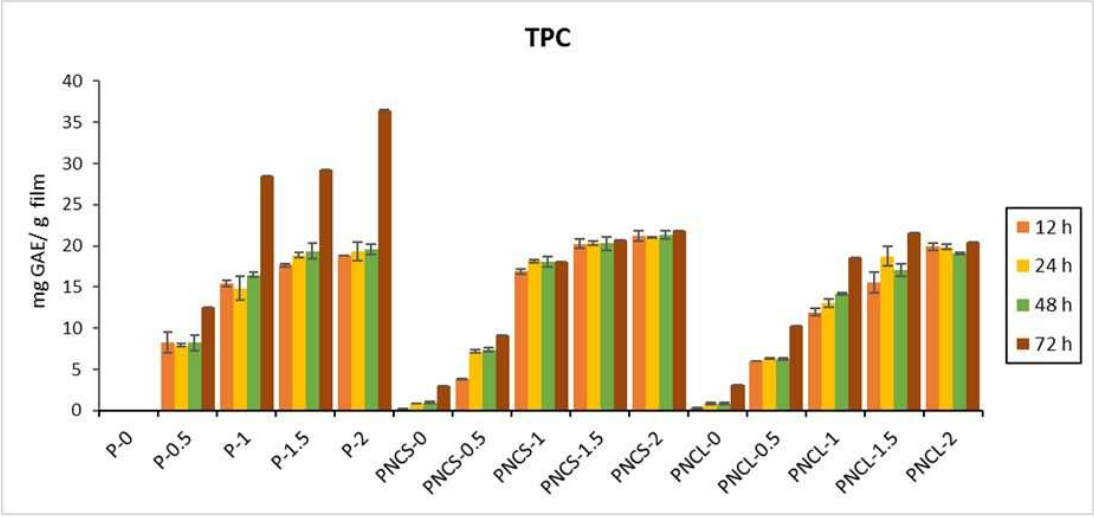

Figure 5. Total phenolic compounds (TPC) of the films at different time. The values were average ± standard deviation (n = 3).

In Figure 5 when comparing the films with shrimp and lobster nanocrystals (PNCS and PNCL), it was observed that the films prepared with shrimp nanocrystals showed slightly higher values of TPC for all release times, in particular for PNCS-1 film. On the other hand, the release of phenolic compound over the time for the films PNCS-1.5 and PNCS-2 was practically constant, keeping its values constant around 20 and 21 mg GAE /g film, respectively. Interestingly, the materials made of shrimp nanocrystals showed better results than the unfilled films over the first 48 h, and then the nanocomposite films made of lobster shrimp over the 72 h.

Figure 6 shows the antioxidant activity of the films obtained by DPPH assay. Among all materials, the antioxidant activity of P-2 film reflected the highest value after 72 h (2.12 ± 0.02 μmol TE/g film). In the films made of PVA and OEO, an important increase in the antioxidant activity was observed from 12 to 72h. The higher growth occurred in the P-1 film with an increase of around 86%. The nanocomposite films made of shrimp nanocrystals showed better results than the nanocomposites prepared with lobster nanocrystals, but just the samples PNCS-1.5 and PNCS-2 over the first 48h.

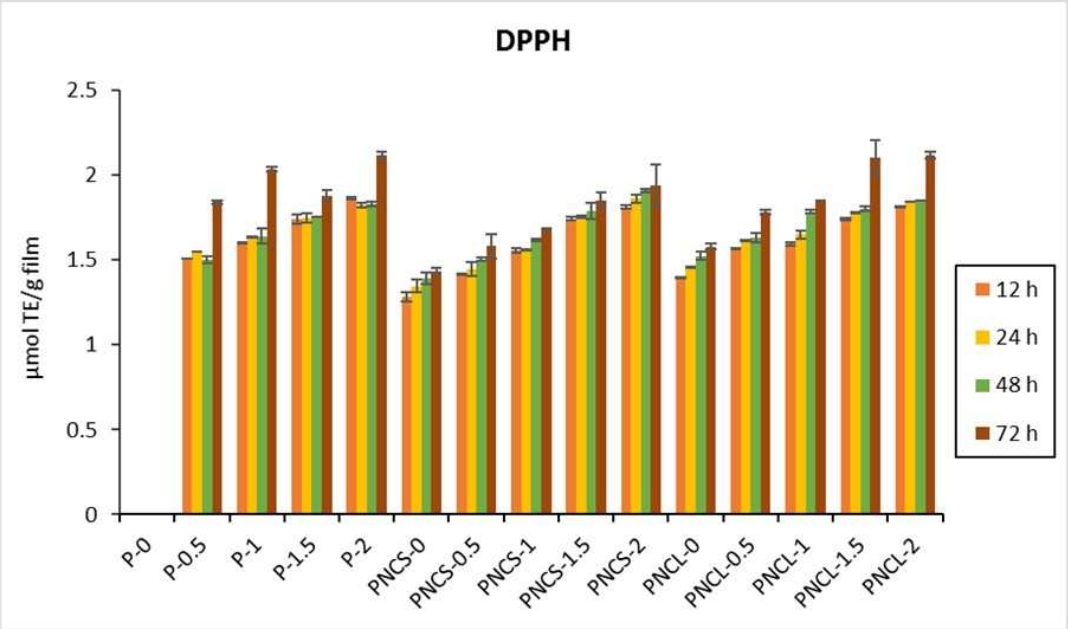

Figure 6. DPPH (2,2-diphenyl-1-picrylhydrazyl) radical scavenging assay of the films at different times. The values were the average ± standard deviation (n = 3).

In general, films containing nanocrystals (PNCS and PNCL) showed a slow release of antioxidant compounds over time (more constant release compared with unfilled films). There are different hypothesis that could explain this fact: (i) chitin nanocrystals create sinuous paths in the PVA matrix and makes that the antioxidant molecules of the OEO take longer to pass through these paths; (ii) the formation of strong interactions between nanocrystals and OEO compounds, making their release slow and constant; (iii) by adding chitin nanocrystals, the porosity of the PVA matrix decreases and therefore, there is a reduction in the segmental mobility of the OEO; and (iv) chitin nanocrystals form a network and, in addition, increase the crystallinity of PVA molecules and this obstructs the mobility of OEO molecules [51,52].

4. Conclusion

The main aim of this study was to evaluate the effect of the incorporation of α-chitin nanocrystals from shrimp and lobster on the final properties PVA/OEO films made by solvent casting.

Our data demonstrated that the nanocomposite films were homogeneous and translucent even with a slight increase of the opacity. Nonetheless, the obtained nanocomposite films containing α-CHNC showed: (i) better thermal stability; (ii) better mechanical properties. Moreover, after exposure the nanocomposite films to UV radiation, it was demonstrated that the presence of α-CHNC had a retarding effect on their loss of mechanical properties; (iii) a more constant release of the antioxidant compounds over time for both TPC and DPPS assays; (iv) better antioxidant activity for the materials made of shrimp nanocrystals over the first 48h; and (v) no major effects were found regarding the source of chitin.

These results demonstrated that the nanocomposites films of PVA, α-CHNC and OEO could be promising biodegradable and active films for the food industry.

Acknowledgments

The authors would like to acknowledge the financial support of the Department of Education of the Basque Government (IT1008-16). Rut Fernández-Marín would like to express her gratitude to the Department of Economic Development and Infrastructures of the Basque Government (scholarship of young researchers training) for supporting financially this research. The authors would like to thank for technical and human support provided by SGIker (UPV/EHU/ERDF, EU). SCMF is the recipient of an E2S UPPA Partnership Chair MANTA (Marine Materials) supported by the 'Investissements d'Avenir' French programme managed by ANR (ANR-16-IDEX-0002), by the Région Nouvelle-Aquitaine and by the Communauté d'Agglomération du Pays Basque.

References

[1] S. Zhao, T. Wang, L. Zhu, P. Xu, X. Wang, L. Gao, D. Li, Analysis of suspended microplastics in the Changjiang Estuary : Implications for riverine plastic load to the ocean, Water Res. 161 (2019) 560–569. https://doi.org/10.1016/j.watres.2019.06.019.

[2] M. Rinaudo, Chitin and chitosan : Properties and applications, Prog. Polym. Sci. 31 (2006) 603–632. https://doi.org/10.1016/j.progpolymsci.2006.06.001.

[3] Y. Ruiz-Navajas, M. Viuda-Martos, E. Sendra, J.A. Perez-Alvarez, J. Fernández-López, In vitro antibacterial and antioxidant properties of chitosan edible fi lms incorporated with Thymus moroderi or Thymus piperella essential oils, Food Control. 30 (2013) 386–392. https://doi.org/10.1016/j.foodcont.2012.07.052.

[4] J. Zeng, Y. He, S. Li, Y. Wang, Chitin Whiskers : An Overview, Bio Macromol. (2012). https://doi.org/10.1021/bm201564a.

[5] A.M. Salaberria, R.H. Diaz, J. Labidi, S.C.M. Fernandes, Role of chitin nanocrystals and nanofibers on physical, mechanical and functional properties in thermoplastic starch films1. Food Hydrocoll. 46 (2015) 93–102. https://doi.org/10.1016/j.foodhyd.2014.12.016.

[6] A.M. Salaberria, S.C.M. Fernandes, R.H. Diaz, J. Labidi, Processing of α-chitin nanofibers by dynamic high pressure homogenization: Characterization and antifungal activity against A. niger, Carbohydr. Polym. 116 (2015) 286–291. https://doi.org/10.1016/j.carbpol.2014.04.047.

[7] A.M. Salaberria, J. Labidi, S.C.M. Fernandes, Chitin nanocrystals and nanofibers as nano-sized fillers into thermoplastic starch-based biocomposites processed by

melt-mixing, Chem. Eng. J. 256 (2014) 356–364. https://doi.org/10.1016/j.cej.2014.07.009.

[8] A. Morales, M.Á. Andrés, J. Labidi, P. Gullón, Industrial Crops & Products UV – vis protective poly (vinyl alcohol)/ bio-oil innovative fi lms, Ind. Crop. Prod. 131 (2019) 281–292. https://doi.org/10.1016/j.indcrop.2019.01.071.

[9] C. Chen, Z. Xu, Y. Ma, J. Liu, Q. Zhang, Properties , vapour-phase antimicrobial and antioxidant activities of active poly (vinyl alcohol) packaging fi lms incorporated with clove oil, Food Control. 88 (2018) 105–112. https://doi.org/10.1016/j.foodcont.2017.12.039.

[10] K.K. Gaikwad, J.Y. Lee, Y.S. Lee, Development of polyvinyl alcohol and apple pomace bio-composite film with antioxidant properties for active food packaging application, J. Food Sci. Technol. 53 (2016) 1608–1619. https://doi.org/10.1007/s13197-015-2104-9.

[11] S. Manso, D. Pezo, R. Gómez-Lus, C. Nerín, Diminution of aflatoxin B1 production caused by an active packaging containing cinnamon essential oil, Food Control. 45 (2014) 101–108. https://doi.org/10.1016/j.foodcont.2014.04.031.

[12] A. El Asbahani, K. Miladi, W. Badri, M. Sala, E.H.A. Addi, H. Casabianca, A. El Mousadik, D. Hartmann, A. Jilale, F.N.R. Renaud, A. Elaissari, C.B. Lyon, Essential oils : From extraction to encapsulation, Int. J. Pharm. 483 (2015) 220–243. https://doi.org/10.1016/j.ijpharm.2014.12.069.

[13] R. Ribeiro-santos, M. Andrade, ScienceDirect Application of encapsulated essential oils as antimicrobial agents in food packaging, Curr. Opin. Food Sci. 14 (n.d.) 78–84. https://doi.org/10.1016/j.cofs.2017.01.012.

[14] R. Ribeiro-Santos, M. Andrade, N.R. de Melo, A. Sanches-Silva, Use of essential oils in active food packaging: Recent advances and future trends, Trends Food Sci. Technol. 61 (2017) 132–140. https://doi.org/10.1016/j.tifs.2016.11.021.

[15] H. Baydar, O. Sagdic, G. Özkan, T. Karadogan, Antibacterial activity and composition of essential oils from Origanum , Thymbra and Satureja species with commercial importance in Turkey, Food Control. 15 (2004) 169–172. https://doi.org/10.1016/S0956-7135(03)00028-8.

[16] S. Hosseini Fakhreddin, M. Zandi, M. Rezaei, F. Farahmandghavi, Two-step method for encapsulation of oregano essential oil in chitosan nanoparticles : Preparation , characterization and in vitro release study, Carbohydr. Polym. 95 (2013) 50–56. https://doi.org/10.1016/j.carbpol.2013.02.031.

[17] Á. Perdones, M. Vargas, L. Atarés, A. Chiralt, Food Hydrocolloids Physical , antioxidant and antimicrobial properties of chitosan e cinnamon leaf oil fi lms as affected by oleic acid, Food Hydrocoll. 36 (2014) 256–264. https://doi.org/10.1016/j.foodhyd.2013.10.003.

[18] S. Sahraee, J.M. Milani, B. Ghanbarzadeh, H. Hamishehkar, LWT - Food Science and Technology Effect of corn oil on physical , thermal , and antifungal properties of gelatin-based nanocomposite fi lms containing nano chitin, LWT - Food Sci. Technol. 76 (2017) 33–39. https://doi.org/10.1016/j.lwt.2016.10.028.

[19] F. Duman, M. Kaya, International Journal of Biological Macromolecules Crayfish chitosan for microencapsulation of coriander (Coriandrum sativum L .) essential oil, Int. J. Biol. Macromol. 92 (2016) 125–133. https://doi.org/10.1016/j.ijbiomac.2016.06.068.

[20] H. Chi, S. Song, M. Luo, C. Zhang, W. Li, L. Li, Y. Qin, Scientia Horticulturae E

ff ect of PLA nanocomposite fi lms containing bergamot essential oil , TiO 2 nanoparticles , and Ag nanoparticles on shelf life of mangoes, Sci. Hortic. (Amsterdam). 249 (2019) 192–198. https://doi.org/10.1016/j.scienta.2019.01.059.

[21] X. Chen, X. He, B. Zhang, X. Fu, J. Jane, Q. Huang, International Journal of Biological Macromolecules Effects of adding corn oil and soy protein to corn starch on the physicochemical and digestive properties of the starch, Int. J. Biol. Macromol. 104 (2017) 481–486.

[22] M. Ahmad, S. Benjakul, T. Prodpran, T. Winarni, Food Hydrocolloids Physico-mechanical and antimicrobial properties of gelatin fi lm from the skin of unicorn leatherjacket incorporated with essential oils, Food Hydrocoll. 28 (2012) 189–199. https://doi.org/10.1016/j.foodhyd.2011.12.003.

[23] K. Munhuweyi, O.J. Caleb, C.L. Lennox, A.J. Van Reenen, U. Linus, Postharvest Biology and Technology In vitro and in vivo antifungal activity of chitosan-essential oils against pomegranate fruit pathogens, Postharvest Biol. Technol. 129 (2017) 9–22. https://doi.org/10.1016/j.postharvbio.2017.03.002.

[24] J. Wu, S. Ge, H. Liu, S. Wang, S. Chen, J. Wang, J. Li, Q. Zhang, ScienceDirect Properties and antimicrobial activity of silver carp (Hypophthalmichthys molitrix) skin gelatin-chitosan films incorporated with oregano essential oil for fish preservation, Food Packag. Shelf Life. 2 (2014) 7–16. https://doi.org/10.1016/j.fpsl.2014.04.004.

[25] S. Singh, K.K. Gaikwad, Y.S. Lee, International Journal of Biological Macromolecules Antimicrobial and antioxidant properties of polyvinyl alcohol bio composite films containing seaweed extracted cellulose nano-crystal and basil leaves extract, Int. J. Biol. Macromol. 107 (2018) 1879–1887.

https://doi.org/10.1016/j.ijbiomac.2017.10.057.

[26] C. Chen, Z. Xu, Y. Ma, J. Liu, Q. Zhang, Z. Tang, K. Fu, F. Yang, J. Xie, Properties , vapour-phase antimicrobial and antioxidant activities of active poly (vinyl alcohol) packaging fi lms incorporated with clove oil, Food Control. 88 (2018) 2012–2019.

[27] S.M.B. Hashemi, A.M. Khaneghah, Progress in Organic Coatings Characterization of novel basil-seed gum active edible fi lms and coatings containing oregano essential oil, Prog. Org. Coatings. 110 (2017) 35–41. https://doi.org/10.1016/j.porgcoat.2017.04.041.

[28] A. Fraj, F. Jaâfar, M. Marti, L. Coderch, N. Ladhari, Industrial Crops & Products A comparative study of oregano (Origanum vulgare L .) essential oil-based polycaprolactone nanocapsules / microspheres : Preparation , physicochemical characterization , and storage stability, Ind. Crop. Prod. 140 (2019) 111669. https://doi.org/10.1016/j.indcrop.2019.111669.

[29] S. Ribes, A. Fuentes, J.M. Barat, E ff ect of oregano (Origanum vulgare L . ssp . hirtum) and clove (Eugenia spp .) nanoemulsions on Zygosaccharomyces bailii survival in salad dressings, Food Chem. 295 (2019) 630–636. https://doi.org/10.1016/j.foodchem.2019.05.173.

[30] N. Ardekani Torabi, M. Khorram, K. Zomorodian, S. Yazdanpanah, H. Veisi, V. Hojat, International Journal of Biological Macromolecules Evaluation of electrospun poly (vinyl alcohol) -based nano fi ber mats incorporated with Zataria multi fl ora essential oil as potential wound dressing, Int. J. Biol. Macromol. 125 (2019) 743–750. https://doi.org/10.1016/j.ijbiomac.2018.12.085.

[31] F. Luzi, E. Fortunati, G. Giovanale, A. Mazzaglia, L. Torre, G. Mariano,

International Journal of Biological Macromolecules Cellulose nanocrystals from Actinidia deliciosa pruning residues combined with carvacrol in PVA CH films with antioxidant / antimicrobial properties for packaging applications, Int. J. Biol. Macromol. 104 (2017) 43–55. https://doi.org/10.1016/j.ijbiomac.2017.05.176.

[32] E. Jahed, M.A. Khaledabad, H. Almasi, R. Hasanzadeh, Physicochemical properties of Carum copticum essential oil loaded chitosan films containing organic nanoreinforcements, Carbohydr. Polym. 164 (2017) 325–338. https://doi.org/10.1016/j.carbpol.2017.02.022.

[33] M.R. Kasaai, Determination of the degree of N -acetylation for chitin and chitosan by various NMR spectroscopy techniques : A review, Carbohydr. Polym. 79 (2010) 801–810. https://doi.org/10.1016/j.carbpol.2009.10.051.

[34] F.A. Al Sagheer, M.A. Al-sughayer, S. Muslim, M.Z. Elsabee, Extraction and characterization of chitin and chitosan from marine sources in Arabian Gulf, Carbohydr. Polym. J. 77 (2009) 410–419. https://doi.org/10.1016/j.carbpol.2009.01.032.

[35] R. Priyadarshi, B. Kumar, F. Deeba, A. Kulshreshtha, Food Hydrocolloids Chitosan fi lms incorporated with Apricot (Prunus armeniaca) kernel essential oil as active food packaging material, Food Hydrocoll. 85 (2018) 158–166. https://doi.org/10.1016/j.foodhyd.2018.07.003.

[36] B. Gullón, P. Gullón, T.A. Lú-chau, M. Teresa, J.M. Lema, Industrial Crops & Products Optimization of solvent extraction of antioxidants from Eucalyptus globulus leaves by response surface methodology : Characterization and assessment of their bioactive properties, Ind. Crop. Prod. 108 (2017) 649–659. https://doi.org/10.1016/j.indcrop.2017.07.014.

[37] A.M. Salaberria, R.H. Diaz, J. Labidi, S.C.M. Fernandes, Preparing valuable renewable nanocomposite films based exclusively on oceanic biomass - Chitin nanofillers and chitosan, React. Funct. Polym. 89 (2015) 31–39. https://doi.org/10.1016/j.reactfunctpolym.2015.03.003.

[38] V. Gomes, L. Souza, J.R.A. Pires, P. Freitas, A.A.S. Lopes, F.M.B. Fernandes, M. Paula, I.M. Coelhoso, A. Luisa, Bionanocomposites of chitosan / montmorillonite incorporated with Rosmarinus o ffi cinalis essential oil : Development and physical characterization, Food Packag. Shelf Life. 16 (2018) 148–156. https://doi.org/10.1016/j.fpsl.2018.03.009.

[39] S.R. Kanatt, M.S. Rao, S.P. Chawla, A. Sharma, Food Hydrocolloids Active chitosan e polyvinyl alcohol fi lms with natural extracts, Food Hydrocoll. 29 (2012) 290–297. https://doi.org/10.1016/j.foodhyd.2012.03.005.

[40] C. Chen, J. Xie, F. Yang, H. Zhang, Z.X.J.L.Y. Chen, Development of moisture-absorbing and antioxidant active packaging film based on poly (vinyl alcohol) incorporated with green tea extract and its effect on the quality of dried eel, J. Food Process. Preserv. (2017) 1–11. https://doi.org/10.1111/jfpp.13374.

[41] Z. Yu, B. Li, J. Chu, P. Zhang, Silica in situ enhanced PVA / chitosan biodegradable fi lms for food packages, Carbohydr. Polym. 184 (2018) 214–220. https://doi.org/10.1016/j.carbpol.2017.12.043.

[42] J.-P. Fan, J.-J. Luo, X.-H. Zhang, B. Zhen, C.-Y. Dong, Y. Li, J. Shen, Y.-T. Cheng, H.-P. Chen, A novel electrospun β -CD / CS / PVA nano fi ber membrane for simultaneous and rapid removal of organic micropollutants and heavy metal ions from water, Chem. Eng. J. 378 (2019) 122232. https://doi.org/10.1016/j.cej.2019.122232.

[43] V. Zubillaga, A.M. Salaberria, T. Palomares, A. Alonso-Varona, S. Kootala, J. Labidi, S.C.M. Fernandes, Chitin Nanoforms Provide Mechanical and Topological Cues to Support Growth of Human Adipose Stem Cells in Chitosan Matrices, Biomacromolecules. 19 (2018) 3000–3012. https://doi.org/10.1021/acs.biomac.8b00570.

[44] A.M. Salaberria, R.H. Diaz, J. Labidi, S.C.M. Fernandes, Preparing valuable renewable nanocomposite films based exclusively on oceanic biomass – Chitin nanofillers and chitosan, React. Funct. Polym. 89 (2015) 31–39.

[45] J. Bonilla, T. Poloni, R. V Lourenço, P.J.A. Sobral, Food Bioscience Antioxidant potential of eugenol and ginger essential oils with gelatin / chitosan fi lms ☆, Food Biosci. J. 23 (2018) 107–114. https://doi.org/10.1016/j.fbio.2018.03.007.

[46] S. Yoon, Y. Kim, B. Il, J. Je, Journal of Photochemistry & Photobiology , B : Biology Preparation and antibacterial activities of chitosan-gallic acid / polyvinyl alcohol blend fi lm by LED-UV irradiation, J. Photochem. Photobiol. B Biol. 176 (2017) 145–149. https://doi.org/10.1016/j.jphotobiol.2017.09.024.

[47] J. Rodríguez, M.J. Martín, M.A. Ruiz, B. Clares, Current encapsulation strategies for bioactive oils: From alimentary to pharmaceutical perspectives, Food Res. Int. 83 (2016) 41–59. https://doi.org/10.1016/j.foodres.2016.01.032.

[48] Y. Bai, Y. Zhao, Y. Li, J. Xu, X. Fu, X. Gao, X. Mao, Z. Li, UV-shielding alginate films crosslinked with Fe3+ containing EDTA, Carbohydr. Polym. (2019) 115–480. https://doi.org/10.1016/j.carbpol.2019.115480.

[49] J. Hafsa, M. ali Smach, M.R. Ben Khedher, B. Charfeddine, K. Limem, H. Majdoub, S. Rouatbi, Physical, antioxidant and antimicrobial properties of

chitosan films containing Eucalyptus globulus essential oil, LWT - Food Sci. Technol. 68 (2016) 356–364. https://doi.org/10.1016/j.lwt.2015.12.050.

[50] E. Jahed, M. Alizadeh, H. Almasi, R. Hasanzadeh, Physicochemical properties of Carum copticum essential oil loaded chitosan films containing organic nanoreinforcements, Carbohydr. Polym. 164 (2017) 325–338. https://doi.org/10.1016/j.carbpol.2017.02.022.

[51] H. Almasi, B. Ghanbarzadeh, J. Dehghannya, A.A. Entezami, Food Additives & Contaminants : Part A Development of a novel controlled-release nanocomposite based on poly (lactic acid) to increase the oxidative stability of soybean oil, Food Addit. Contam. Part A. 31 (2014) 1586–1597. https://doi.org/10.1080/19440049.2014.935962.

[52] E. Jahed, M.A. Khaledabad, H. Almasi, R. Hasanzadeh, Physicochemical properties of Carum copticum Essential Oil Loaded Chitosan Films Containing Organic Nanoreinforcements, Carbohydr. Polym. 164 (2017) 325–338. https://doi.org/10.1016/j.carbpol.2017.02.022.